The Journal of Immunology

B Cell–Intrinsic CD84 and Ly108 Maintain Germinal Center B Cell Tolerance

Eric B. Wong, Chetna Soni, Alice Y. Chan, Phillip P. Domeier, Shwetank, Thomas Abraham, Nisha Limaye, Tahsin N. Khan, Melinda J. Elias, Sathi Babu Chodisetti, Edward K. Wakeland and Ziaur S. M. Rahman

J Immunol 2015; 194:4130-4143; Prepublished online 23 March 2015;
doi: 10.4049/jimmunol.1403023
http://www.jimmunol.org/content/194/9/4130

The Journal of Immunology is published twice each month by
The American Association of Immunologists, Inc.,
9650 Rockville Pike, Bethesda, MD 20814-3994.

Print ISSN: 0022-1767 Online ISSN: 1550-6606.

B Cell–Intrinsic CD84 and Ly108 Maintain Germinal Center B Cell Tolerance

Eric B. Wong,* Chetna Soni,* Alice Y. Chan,[†,1] Phillip P. Domeier,* Shwetank,* Thomas Abraham,[‡] Nisha Limaye,[†,2] Tahsin N. Khan,*[,3] Melinda J. Elias,* Sathi Babu Chodisetti,* Edward K. Wakeland,[†] and Ziaur S. M. Rahman*

Signaling lymphocyte activation molecules (SLAMs) play an integral role in immune regulation. Polymorphisms in the SLAM family receptors are implicated in human and mouse model of lupus disease. The lupus-associated, somatically mutated, and class-switched pathogenic autoantibodies are generated in spontaneously developed germinal centers (GCs) in secondary lymphoid organs. The role and mechanism of B cell–intrinsic expression of polymorphic SLAM receptors that affect B cell tolerance at the GC checkpoint are not clear. In this study, we generated several bacterial artificial chromosome–transgenic mice that overexpress C57BL/6 (B6) alleles of different SLAM family genes on an autoimmune-prone B6.*Sle1b* background. B6.*Sle1b* mice overexpressing B6-derived Ly108 and CD84 exhibit a significant reduction in the spontaneously developed GC response and autoantibody production compared with B6.*Sle1b* mice. These data suggest a prominent role for *Sle1b*-derived Ly108 and CD84 in altering the GC checkpoint. We further confirm that expression of lupus-associated CD84 and Ly108 specifically on GC B cells in B6.*Sle1b* mice is sufficient to break B cell tolerance, leading to an increase in autoantibody production. In addition, we observe that B6.*Sle1b* B cells have reduced BCR signaling and a lower frequency of B cell–T cell conjugates; the reverse is seen in B6.*Sle1b* mice overexpressing B6 alleles of CD84 and Ly108. Finally, we find a significant decrease in apoptotic GC B cells in B6.*Sle1b* mice compared with B6 controls. Our study establishes a central role for GC B cell–specific CD84 and Ly108 expression in maintaining B cell tolerance in GCs and in preventing autoimmunity. *The Journal of Immunology*, 2015, 194: 4130–4143.

The signaling lymphocyte activation molecule (SLAM) family receptors play critical roles in immune regulation and are required for an effective humoral response (1, 2). The *Sle1b* sublocus derived from the lupus-prone NZM2410/NZW strain harbors the SLAM family (*Slamf*) genes (3). Previous studies suggested that *Slamf* genes are major players in mediating the loss of tolerance to nuclear Ags and in the development of autoimmunity in C57BL/6 (B6).*Sle1b* mice (3). Polymorphisms in the Ly108/Slamf6 gene are implicated in the loss of early B cell–mediated (4), as well as peripheral T cell–mediated, tolerance (5). Several independent studies suggested the contribution of three other SLAMF genes, *Slamf1* (SLAM/CD150), *Slamf2* (CD48), and *Slamf3* (Ly9), in autoimmunity (6–8). However, the role of B cell–intrinsic expression of different isoforms of Ly108 or other SLAM receptors in the regulation of B cell tolerance at the germinal center (GC) checkpoint remains unclear. Elucidation of the mechanism by which SLAM receptors regulate GCs is important, because GCs develop spontaneously in autoimmune mice and humans and generate somatically mutated and class-switched pathogenic autoantibodies (9–11).

Because *Slamf* genes are genetically linked, it has been difficult to determine the potential role of polymorphisms in a specific family member in autoimmunity using knockout mice generated in an autoimmune 129 background and subsequently backcrossed to B6 mice (6–8, 12, 13). It is also unclear whether non-*Slamf* genes located in *Sle1b* contribute to a break in B cell tolerance given the presence of nonsynonymous mutations in these genes in autoimmune B6.*Sle1b* mice (3). To definitively determine the role of particular *Slamf* and/or non-*Slamf* genes within the *Sle1b* sublocus in the development of autoimmunity and to study the mechanisms by which these genes affect B cell tolerance at the GC checkpoint, we used a bacterial artificial chromosome (BAC)-transgenic rescue approach. We generated six BAC-transgenic mouse lines expressing B6 alleles of the different genes spanning the entire *Sle1b* sublocus and then bred them onto B6.*Sle1b* mice. The B6.*Sle1b* BAC-transgenic mouse line containing B6 alleles of Ly108 and CD84 (designated *Sle1b*-BAC90) showed a significant reduction in anti-nuclear Ab (ANA) titers and positivity (penetrance) and a decreased spontaneously developed GC (Spt-GC) response, indicating a critical role for Ly108 and CD84 in maintaining GC B cell tolerance.

*Department of Microbiology and Immunology, Pennsylvania State University College of Medicine, Hershey, PA 17033; [†]Department of Immunology, University of Texas Southwestern Medical Center, Dallas, TX 75390; and [‡]Department of Research Resources, Pennsylvania State University College of Medicine, Hershey, PA 17033

[1]Current address: Department of Pediatrics, University of California San Francisco, San Francisco, CA.

[2]Current address: Laboratory of Human Molecular Genetics, de Duve Institute, Université Catholique de Louvain, Brussels, Belgium.

[3]Current address: Department of Molecular Microbiology and Immunology, Oregon Health and Science University, Portland, OR.

Received for publication December 3, 2014. Accepted for publication February 16, 2015.

This work was supported by National Institutes of Health Grant AI091670 (to Z.S.M.R.).

Address correspondence and reprint requests to Dr. Ziaur S.M. Rahman, Department of Microbiology and Immunology, H107, Pennsylvania State University College of Medicine, 500 University Drive, Hershey, PA 17033-0850. E-mail address: zrahman@hmc.psu.edu

The online version of this article contains supplemental material.

Abbreviations used in this article: AFC, Ab-forming cell; ANA, anti-nuclear Ab; B6, C57BL/6; BAC, bacterial artificial chromosome; BM, bone marrow; 2D, two dimensional; ECAR, extracellular acidification rate; GC, germinal center; HEL, hen egg lysozyme; OCR, oxygen consumption rate; PI, propidium iodide; PNA, peanut agglutinin; SA, streptavidin; SAP, SLAM adaptor; SLAM, signaling lymphocyte activation molecule; Sm/RNP, Smith/ribonucleoprotein; Spt-GC, spontaneously developed GC; Tfh cell, follicular helper T cell.

www.jimmunol.org/cgi/doi/10.4049/jimmunol.1403023

Both CD84 and Ly108 are essential in maintaining tolerance because B6.*Sle1b* BAC-transgenic mice expressing the B6 allele of Ly108 alone showed only a partial restoration of tolerance to ANA. Using a conditional deletion (Cre-LoxP) system, we showed that GC B cell–specific expression of autoimmune-prone CD84 and Ly108 genes is sufficient for the loss of B cell tolerance. B cell function assays revealed that polymorphisms in the CD84 and Ly108 proteins in B6.*Sle1b* B cells helped B cells escape tolerance by lowering BCR signaling, decreasing apoptosis, and attenuating B cell–T cell interactions. Normalization of B6.*Sle1b*-derived CD84 and Ly108 by overexpression of wild-type CD84 and Ly108 restored BCR signaling and B cell–T cell interactions. Our results highlight the vital role of GC B cell–specific Ly108 and CD84 expression and function in the maintenance of B cell tolerance at the GC checkpoint.

Materials and Methods

Mice

Breeding pairs of B6, GC B cell Cre (C.129P2[Cg]-*Ighg1*$^{tm1[IRES\text{-}cre]Cgn}$/J), and OT-II–transgenic (B6.Cg-Tg [TcraTcrb]425Cbn/J) mice were originally purchased from The Jackson Laboratory, and mice were bred in-house. Derivation of B6 mice congenic for the *Sle1b* sublocus (named B6.*Sle1b*) was described previously (14). All animals were housed in the specific pathogen–free animal facility at Penn State Hershey Medical Center, and all procedures were performed in accordance with the guidelines approved by the Pennsylvania State University College of Medicine Institutional Animal Care and Use Committee.

Generation of BAC-transgenic mice

BACs were identified from the B6-derived BAC library (BACPAC Resources, Oakland, CA). The following BACs were used: RPCI-23 194D6 (BAC41), RPCI-23 48O11 (BAC47), RPCI-23 171K8 (BAC25), RPCI-23 145F9 (BAC40), RPCI-23–388C4 (BAC90), RPCI-23 462J8 (BAC95), and RPCI-23 438K9 (BAC-Ly108). Bacterial cultures from these BAC clones were grown in Luria broth with chloramphenicol (12.5 μg/ml) overnight at 37˚C. QIAGEN Midi Kit solutions, P1, P2, and P3, were used to isolate BAC DNA (QIAGEN, Valencia, CA). The DNA was purified further by phenol-chloroform extraction, followed by cesium chloride gradient ultracentrifugation. BAC DNA was diluted to 50 ng/μl in 10 mM Tris-HCl [pH 7.5] and 0.1 mM EDTA and injected into fertilized oocytes derived from B6 mice. Founder lines were identified by PCR specific for the vector ends and then bred onto the respective genetic backgrounds.

Generation of floxed BAC90 mice

The BAC (RPCI-23–388C4) used to generate floxed BAC90 mice was purchased from BACPAC Resources. The BAC vector backbone already contained LoxP sites that flanked the insert (B6-derived CD84 and Ly108). No additional manipulation was made to the backbone. BAC vector DNA amplification, purification, and injection into B6-derived fertilized oocytes were performed as described above ("Generation of BAC-transgenic mice").

Flow cytometry

The following Abs were used for flow cytometric analysis of mouse splenocytes or bone marrow (BM) cells. Pacific Blue–anti-B220 (RA3-6B2), Alexa Fluor 700–anti-CD4 (RM4-5), PE–anti-PD-1 (29F.1A12), PerCP–Cy5.5–anti-CD69 (H1.2F3), allophycocyanin–Cy7–anti-CD25 (PC61), Cy5–anti-CD86 (GL1), PE-Cy7–anti-CD95 (FAS, Jo2), PE-Cy7–anti-MHC class II (M5/114.15.2), allophycocyanin–anti-CD24 (HSA) (M1/69), biotin–anti-Ly5.1 (BP-1) (6C3), FITC–anti-CD23 (B3B4), and PE–Cy5–streptavidin (SA) were from purchased from BioLegend (San Diego, CA). Biotin–anti-CXCR5 (2G8) was purchased from BD Pharmingen (San Diego, CA). FITC–peanut agglutinin (PNA) was purchased from Vector Labs (Burlingame, CA). PE–anti-IgM (eB121-15F9), allophycocyanin anti-CD93 (AA4.1), and FITC–anti-F4/80 (BM8) were purchased from eBioscience (San Diego, CA). The following Abs were used for phosphoflow analysis of purified mouse B cells: PE–anti-Btk (pY223)/ItK (pY180) (N35-86), Alexa Fluor 647–anti-ERK1/2 (pT202/pY204) (20A), Pacific Blue–anti-p38 MAPK (pT180/pY182), and Alexa Fluor 488–anti-Syk (pY348) (I120-722). Stained cells were analyzed using a BD LSR II flow cytometer (BD Biosciences, Franklin Lakes, NJ). Data were acquired using FACSDiva software (BD Biosciences, San Jose, CA) and analyzed using FlowJo software (TreeStar, San Carlos, CA).

Immunohistology

The following Abs and reagents were used for immunohistochemical analysis of mouse spleen sections: PE–anti-CD4 (GK1.5), FITC-GL7, and allophycocyanin–anti-IgD (all from BD Biosciences). Spleen cryostat sections (5–6 μm) were prepared as previously described (15). Immunohistochemistry was performed as described (15), and stained sections were analyzed with a Leica DM4000 fluorescence microscope and Leica software (Leica Microsystems, Buffalo Grove, IL). The color intensity of the images was enhanced slightly using Adobe Photoshop CS4 (Adobe Systems, San Jose, CA) for better visualization; it was carried out consistently among all sections while maintaining the integrity of the data.

ELISPOT assays

ELISPOT assays were performed as previously described (16). Briefly, splenocytes in 10% RPMI 1640 were plated at a concentration of 1×10^5 cells/well onto anti-IgM–coated or anti-IgG–coated (Invitrogen, Grand Island, NY) multiscreen 96-well filtration plates or at a concentration of 1×10^6 cells/well on dsDNA-, histone-, or nucleosome-coated multiscreen 96-well filtration plates (Millipore, Bedford, MA). Serially diluted (1:2) cells were incubated for 6 h at 37˚C. IgM-producing Ab-forming cells (AFCs) were detected using biotinylated anti-mouse IgM (Jackson ImmunoResearch, West Grove, PA) and SA–alkaline phosphatase (Vector Laboratories, Burlingame, CA). IgG-producing AFCs were detected using alkaline phosphatase–conjugated anti-mouse IgG (Molecular Probes, Grand Island, NY). dsDNA-, histone-, and nucleosome-specific AFCs were detected by biotinylated anti-κ Ab (Invitrogen, Grand Island, NY) and SA–alkaline phosphatase (Vector Laboratories) or alkaline phosphatase–conjugated anti-mouse IgG (Molecular Probes, Grand Island, NY). Plates were developed using the Vector Blue AP Substrate Kit III (Vector Laboratories). ELISPOTs were enumerated and analyzed using a computerized imaging/analysis system (Cellular Technology, Shaker Heights, OH).

Serology: Ig and autoantibody titers

ELISA plates were coated with anti-IgM or anti-IgG capture Abs (Invitrogen) and detected using biotinylated anti-mouse IgM (Jackson ImmunoResearch) or alkaline phosphatase–conjugated anti-mouse IgG (Molecular Probes). Total IgG autoantibody titers were measured in ELISA plates coated with dsDNA, histone, nucleosome, Smith/ribonucleoprotein (Sm/RNP), or cardiolipin and detected with biotinylated anti-κ Ab (Invitrogen). IgG subtype-specific autoantibody titers were detected by biotinylated IgG1, biotinylated IgG2b, and alkaline phosphatase–IgG2c Abs (Southern Biotech, Birmingham, AL). Biotinylated Abs were detected by SA–alkaline phosphatase (Vector Laboratories). The plates were developed using PNPP (disodium salt; Thermo Fisher Scientific, Rockford, IL) substrates for alkaline phosphatase.

In vitro B cell–proliferation assay

Naive B cells were purified from the indicated mice with mouse anti-CD43 (Ly-48) MicroBeads. Purified B cells were stained with 3 μM CFSE (Sigma-Aldrich, St. Louis, MO) in PBS with 5% FBS for 15 min at room temperature. Stained B cells were cultured with 25 μg/ml soluble anti-IgM (Jackson ImmunoResearch) and 20 μg/ml soluble anti-CD40 Ab (BioLegend). After 72 h of stimulation, cells were acquired using a BD LSR II flow cytometer.

Ex vivo apoptosis–detection assay

Total splenocytes from 3–4-mo-old female mice of the indicated strains were stained in vitro with SR FLICA Poly Caspase detection reagent (AbD Serotec, Kidlington, U.K.) for 30 min at 37˚C in a water bath, followed by staining with the indicated GC B cell markers. Cells were acquired immediately after staining on the BD LSR II cytometer. DAPI$^+$ dead cells and doublets were gated out during the analysis.

Cell cycle analysis

B cells were cultured with anti-IgM (25 μg/ml) and anti-CD40 (20 μg/ml) for the indicated times, harvested, washed with chilled PBS, and fixed with chilled 70% ethanol overnight at −20˚C. Subsequently, cells were centrifuged at 1000 × *g* for 10 min at 4˚C, washed with PBS, and stained with propidium iodide (PI) staining solution, containing 50 μg/ml PI, 50 μg/ml RNase A (Roche Applied Sciences, Indianapolis, IN), and 100 μM EDTA in PBS, for 1–2 h at 42˚C. Cells were analyzed by flow cytometry.

Calcium flux assay

Naive B cells were purified from each group of mice with mouse anti-CD43 (Ly-48) MicroBeads. Purified B cells were stained with Fura Red (10 μM)

and Fluo-3 (5 μM) (Invitrogen) in dyeless RPMI 1640 (Mediatech) for 45 min at 37˚C. A baseline calcium reading was acquired for 1 min before the addition of 5 or 10 μg/ml anti-IgM (Jackson ImmunoResearch), followed immediately by a 3-min acquisition through the BD LSR II flow cytometer.

B cell–T cell in vitro conjugate assay

Naive B cells from each indicated group of mice were purified with mouse anti-CD43 (Ly-48) MicroBeads, stained with 5 μM CellTrace Violet (Invitrogen), and activated with 25 μg/ml soluble anti-IgM and 1 μg/ml LPS for 24 h at 37˚C. Naive T cells from OT-II–transgenic mice were purified with a pan-T isolation kit (Miltenyi Biotec), stained with 3 μM CFSE, and activated with 10 μg/ml anti-CD3 and 2 μg/ml anti-CD28 for 24 h at 37˚C. A total of 10 μg/ml OVA peptide (InvivoGen, San Diego, CA) was added to the B cells 3 h prior to the start of the assay. A total of 1×10^6 B cells and 1×10^6 T cells were placed together for the stipulated times, fixed with 4% paraformaldehyde, and acquired using a BD LSR II.

Phosphoflow analysis

Splenocytes isolated from each indicated mouse group were activated with 25 μg/ml anti-IgM for the indicated times at 37˚C. Following activation, cells were fixed with Lyse/Fix (BD) for 10 min at 37˚C. Following washes, cells were permeabilized with Perm/Wash Buffer (BD) for 30 min at room temperature. Following two washes with Perm/Wash Buffer, cells were stained for anti-B220 and phosphoflow Abs (BD) described above for 1 h. Samples were acquired using a BD LSR II flow cytometer.

Assessment of GC sizes

Immunohistochemistry was performed using the Abs listed in the "Immunohistology" section, and stained sections were analyzed with a Leica DM4000 fluorescence microscope and Leica software (Leica Microsystems). Ten randomly selected GCs/mouse from the indicated mouse groups (five mice from each group) were assessed for total area (μm^2) using Leica Microsystems software.

In vitro B cell–functional assays

B cells were purified from naive B6, B6.*Sle1b*, or *Sle1b*-BAC90 mice with mouse anti-CD43 (Ly-48) MicroBeads, stimulated with 25 μg/ml anti-IgM, 10 μg/ml anti-CD40, and/or 5 μg/ml anti-Ly108 (13G3-19D) (eBioscience) or 2 μg/ml recombinant CD84 agonist (R&D Systems) for 24 h, and acquired using a BD LSR II flow cytometer.

DNA/RNA preparation and real-time RT-PCR

Total DNA was isolated with a DNeasy Blood and Tissue kit (QIAGEN, Hilden, Germany), following the manufacturer's guidelines, from the tails of the indicated mice. Gene expression was quantified using TaqMan Master Mix and the StepOnePlus Real-Time PCR system (Applied Biosystems, Grand Island, NY). Primers for CD84 and Ly108 copy number assay were purchased from Life Technologies. Amplification conditions for all primer sets were 1 cycle at 95˚C for 10 min, followed by 40 cycles at 95˚C for 15 s and 60˚C for 1 min. Mouse Tert was used as the reference gene.

Total RNA was isolated from purified B cells and T cells or from GC B cells and follicular helper T cells (Tfh cells) sorted with a FACSAria Sorter using the RNeasy Mini Kit (QIAGEN), following the manufacturer's guidelines. RNA was reverse transcribed using the High-Capacity Reverse Transcription kit (Applied Biosystems). Gene expression was quantified using TaqMan PCR Master Mix kit or Power SYBR Green PCR Master Mix Kit using the StepOnePlus Real-Time PCR System (all from Applied Biosystems). Primers for the SLAM genes were purchased from Life Technologies, and Ly108 isoform primers were designed using Primer3 software and synthesized by IDT Technologies (Coralville, Iowa). The following primer sequences were used: Ly108.1: forward 5′-CTCGTCCAATGCAGGAAATG-3′ and reverse 5′-AGATGTGTTCTCCCTGGATTTC-3′; Ly108.2: forward 5′-CTCGTCCAATGCAGGAAATG-3′ and reverse 5′-AGGAGTTATAGTTGATTAAG-3′; and Ly108-H1: forward 5′-AGCACAGATGGCCCAGG-3′, reverse 5′-AGGAGTTATAGTTGATTAAAG-3′. Amplification conditions for all primer sets were 1 cycle at 95˚C for 10 min, followed by 40 cycles at 95˚C for 15 s and 60˚C for 1 min. GAPDH was used as the reference gene for sample normalization.

Extracellular flux analysis

Oxygen consumption rate (OCR) and extracellular acidification rate (ECAR) were measured in a XF96 extracellular flux analyzer using a kit, as per manufacturer's instructions (Seahorse Bioscience, Boston, MA). Briefly, B cells from B6, B6.*Sle1b*, and *Sle1b*-BAC90 mice were purified by negative selection using CD43 MicroBeads by MACS purification (Miltenyi Biotec). Purified B cells were stimulated with 25 μg/ml anti-IgM and 20 μg/ml anti-CD40 for 18 h in RPMI 1640 + 10% FCS. Thereafter, 6×10^5 activated B cells were plated in XF media (Seahorse Bioscience) with 25 mM glucose onto a Cell-Tak (BD Biosciences)-coated XF96 plate. Oligomycin (1 μM), carbonyl cyanide 4- (trifluoromethoxy) phenyl hydrazone (2 μM), rotenone (1 μM), and antimycin (1 μM) were added sequentially, and measurements of extracellular flux were recorded. Glycolysis was calculated from ECAR values at the basal respiration phase, and glycolytic capacity was calculated from ECAR values after the inhibition of ATP synthase by the addition of oligomycin, when cells resort to meeting their energy demands using their maximum glycolytic capacity. OCR and ECAR data were analyzed using Wave software and plotted using GraphPad Prism v6.0 (La Jolla, CA).

Two-dimensional live cell microscopy, image acquisition, and cell-tracking analysis

For the live cell-tracking measurements, the confocal technique (Leica AOBS SP8 laser scanning confocal microscope; Leica Microsystems, Heidelberg, Germany) was used along with a heated live cell stage equipped with a humidified 5% CO_2 perfusion system (TOKAI HIT). The live cell data mode (xyt) in the image-acquisition software (Leica Confocal Software LAF) was used for the two-dimensional (2D) imaging of live cells. Activated B cells loaded with OVA peptide and labeled with CellTrace (Invitrogen) were mixed with activated CFSE-labeled OT-II T cells in 0.5 mg/ml collagen solution, pH 7 (TelCol, type 1 acid-soluble collagen solution from Advanced BioMatrix, San Diego, CA). 2D live cell images of B and T cell contacts were acquired sequentially using the 63×/1.2 high numerical aperture apochromatic water-immersion objective every 30 s for 1 h. The laser lines for excitation included UV diode, 80 MHz white light laser (Leica AOBS SP8 module), and the emission signals were collected sequentially using AOBS tunable filters to eliminate cross-talk and cross-excitation. All of the fluorescent images, as a function of time, were collected using highly sensitive HyD detectors (with time gated option). The images (8 bit) were line-averaged to minimize the random noise, and a pixel format of 512 × 512 was selected. For each sample, 2D time-series images were compiled, and cell tracking was performed using Imaris and Imaris XT (Bitplane, Switzerland) functions, based on the Matlab program. The data were compiled in Microsoft Excel (Microsoft, Redmond, WA) sheets, and final plots, slope measurements, and statistical analysis were performed using GraphPad Prism v6 or Origin Lab v9.1.

Statistical analysis

Unpaired, nonparametric, Mann–Whitney, and Student *t* tests were used for comparing two groups, and one-way ANOVA followed by Tukey's multiple comparison test was used for comparing more than two groups. GraphPad Prism 6 analytical tool (La Jolla, CA) was used for every analysis. Wherever indicated, NS = nonsignificant, $*p \leq 0.05$, $**p \leq 0.01$, $***p \leq 0.001$, and $****p \leq 0.0001$. Error bars reflect mean values, unless otherwise noted.

Results

A major role for SLAM family receptors CD84 and Ly108 in maintaining tolerance

SLAM family genes, located in the telomeric end of chromosome 1 in autoimmune mice (i.e., NZM2410/NZW-derived *Sle1b* interval) and human systemic lupus erythematosus patients, are implicated in altering B cell tolerance (3, 16–18). To definitively determine the contribution of particular *Slamf* genes within the *Sle1b* sublocus in autoimmunity, a panel of B6-derived BACs spanning the entire *Sle1b* interval was used to generate a series of transgenic mouse lines (Fig. 1A).

Multiple founder lines carrying different copy numbers were generated for each BAC (Fig. 1A). Of the six BAC-transgenic mouse lines generated, only the BAC transgene carrying B6 alleles of CD84 and Ly108 (referred to as BAC90) was able to significantly suppress both ANA positivity/penetrance (Fig. 1B) and titers (Fig. 1C) when bred to B6.*Sle1b* mice (referred to as *Sle1b*-BAC90). The BAC transgene carrying 2B4 (*Slamf4*), Ly9 (*Slamf3*), and Cs1 (*Slamf7*) (referred to as BAC25) also had lower ANA titers (Fig. 1C), but 70% of B6.*Sle1b* mice expressing the BAC25 transgene (designated *Sle1b*-BAC25) remained positive for ANA (Fig. 1B). When we analyzed ANA titers in B6.*Sle1b* mice expressing each founder line for a given BAC-transgenic strain, we did not find a significant difference among the

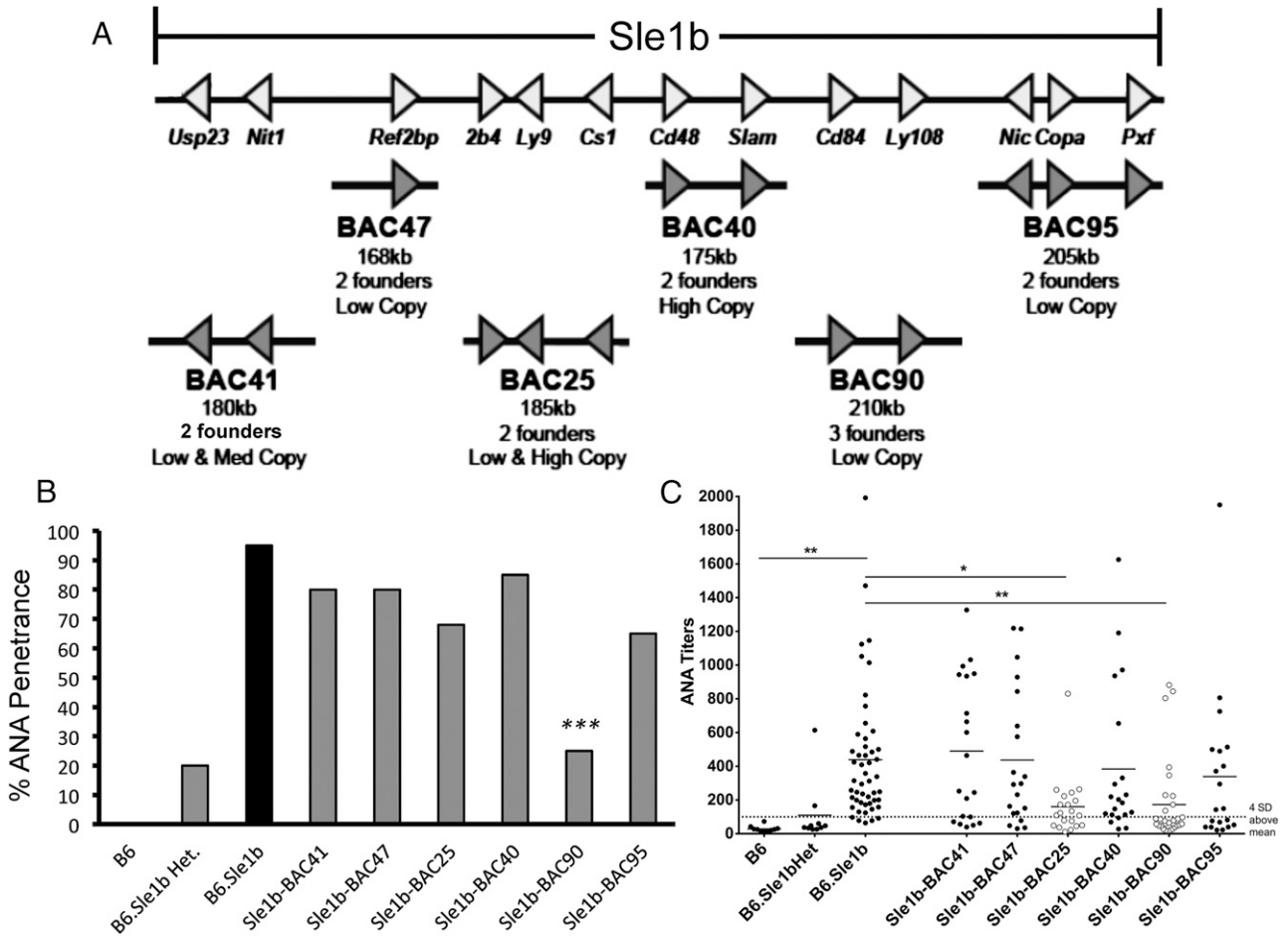

FIGURE 1. Suppression of ANA production in B6.*Sle1b* mice overexpressing B6-derived CD84 and Ly108. (**A**) Schematic diagram of the six B6-derived BACs spanning the *Sle1b* interval. Each BAC harbors B6 alleles that genetically complement the indicated region in the *Sle1b* interval. Founders had variable copy numbers (low copy [1, 2], medium copy [3, 4], and high copy [>10]). (**B**) Six BACs carrying the B6 alleles of the *Sle1b* genes were crossed to B6.*Sle1b* mice, and two or three founder lines for each BAC were analyzed for IgG-specific ANA positivity at 7 mo of age. Statistical analysis was performed using logistic regression (SAS version 9.1). (**C**) IgG ANA titers were assessed in 7-mo-old BAC-transgenic mice. Dotted line represents the value that is four SD above the mean titer from B6 mice. ANA titers in *Sle1b*-BAC25 and *Sle1b*-BAC90 mice (open circles) were significantly higher than in B6.*Sle1b* mice ($p < 0.01$ and $p < 0.001$, respectively). *$p < 0.05$, **$p < 0.01$, ***$p < 0.001$.

individual founder lines, with the exception of BAC25 and BAC90 (Supplemental Fig. 1). Of the three BAC90-transgenic founder lines generated, two (BAC90-4389 and BAC90-4390) had significantly lower ANA titers than the third (BAC90-4270). A significant difference in ANA titers was observed between BAC90-4270 and BAC90-4389 lines (Supplemental Fig. 1). We also observed a difference between the two BAC25 lines (Supplemental Fig. 1).

To determine whether Ly108 alone was able to mediate the suppression of ANA production in *Sle1b*-BAC90 mice, a BAC-transgenic mouse carrying only the B6 allele of Ly108 was generated and bred onto the B6.*Sle1b* background (referred to as *Sle1b*-BAC-Ly108). *Sle1b*-BAC-Ly108 mice displayed a reduction in serum ANA penetrance and titers (Supplemental Fig. 2), but not to the extent that was observed in aged *Sle1b*-BAC90 mice that carry both CD84 and Ly108 (Fig. 1B, 1C). These data indicate that allelic variations in both CD84 and Ly108 were required to break tolerance to nuclear self-Ags in B6.*Sle1b* mice.

Restoration of B cell tolerance at the GC checkpoint by overexpression of B6-derived CD84 and Ly108

Sle1b alters peripheral B cell tolerance at the GC checkpoint, leading to elevated Spt-GC and Tfh cell responses (16). We asked whether introduction of the B6 wild-type alleles of CD84 and Ly108 into B6.*Sle1b* mice could restore tolerance by regulating the GC checkpoint in B6.*Sle1b* mice. We first evaluated the surface expression and found that CD84 and Ly108 levels were higher in B cells from B6.*Sle1b* and *Sle1b*-BAC90 mice compared with B6 mice at 2 mo of age (Supplemental Fig. 3A). However, B6.*Sle1b* B cells exhibited a significant reduction in both CD84 and Ly108 surface expression by 8 mo compared with B6 and *Sle1b*-BAC90 B cells (Supplemental Fig. 3B). A similar temporally biphasic expression profile for CD84 and Ly108 was observed when GC B cells were analyzed at 2 and 8 mo of age (data not shown). CD84 expression on $CD4^+$ T cells remained similar among the three strains, but Ly9 and Ly108 levels on $CD4^+$ T cells were higher in B6.*Sle1b* and *Sle1b*-BAC90 mice than in B6 mice at both 2 and 8 mo of age (data not shown). We observed no difference in SLAM adaptor (SAP) molecule transcript levels in B cells and T cells from these mice (data not shown).

Immunohistological analysis of spleens revealed smaller and less frequent Spt-GCs in B6 and *Sle1b*-BAC90 mice compared with B6.*Sle1b* mice (Fig. 2A, 2B). This decrease in Spt-GCs was confirmed by flow cytometric analysis of splenocytes, which showed a significant reduction in the percentage of $B220^+Fas^{hi}PNA^{hi}$ Spt-GC

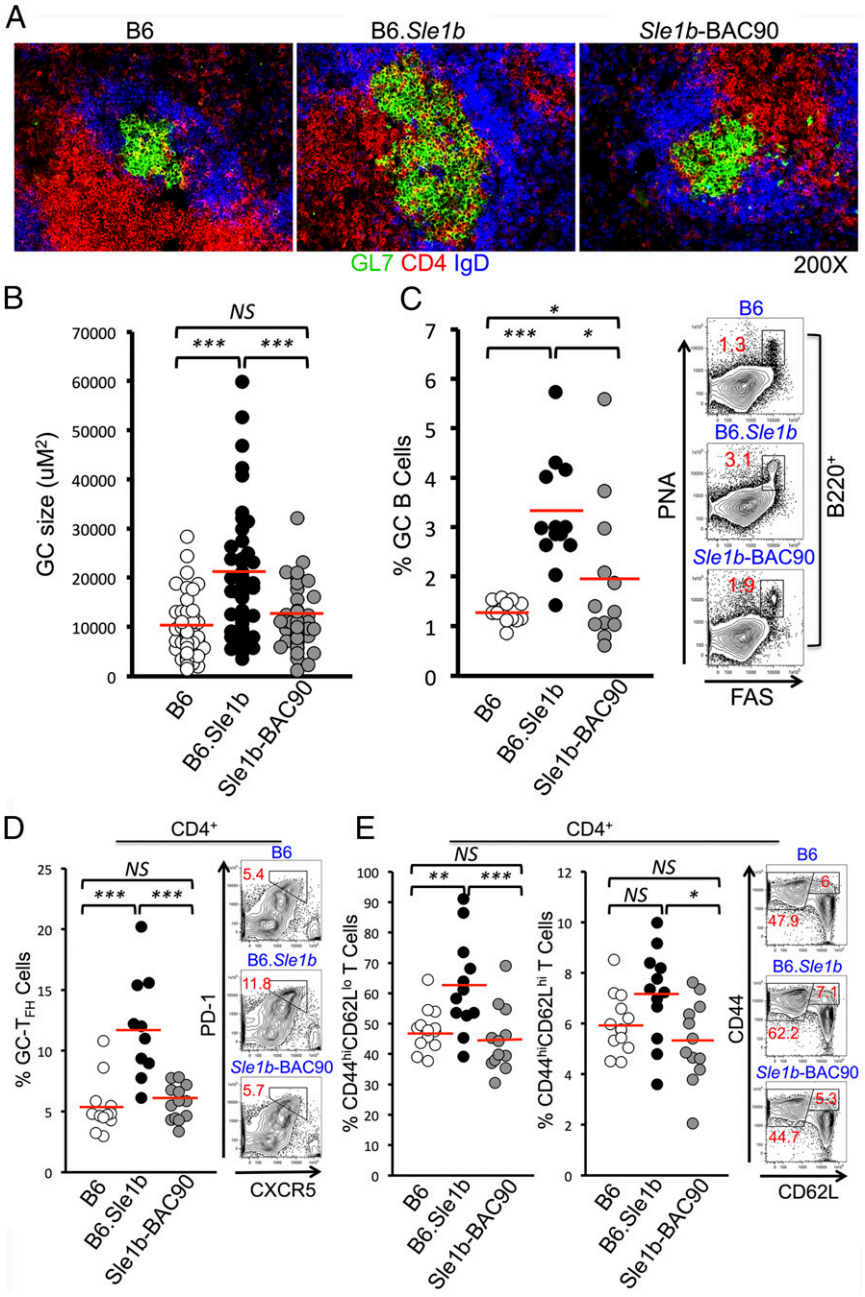

FIGURE 2. Restoration of B cell tolerance in GCs in *Sle1b*-BAC90 mice expressing wild-type CD84 and Ly108. (**A**) Representative immunohistological images of spleen sections from three to five mice/group, stained with GC B cell marker GL7 (green), CD4 T cell marker (red), and follicular B cell marker IgD (blue). (**B**) Scatterplot of the range of GC sizes from each mouse strain. (**C**) Flow cytometric analysis of the percentage of $B220^{+}Fas^{hi}PNA^{hi}$ GC B cells. Each symbol represents an individual mouse. (**D** and **E**) Percentage of Tfh cells ($CD4^{+}CXCR5^{hi}PD\text{-}1^{hi}$), short-lived effector/effector memory T cells ($CD4^{+}CD44^{hi}CD62L^{lo}$), and central memory T cells ($CD4^{+}CD44^{hi}CD62L^{hi}$). Each symbol represents an individual mouse. $*p < 0.05$, $**p < 0.01$, $***p < 0.001$.

B cells in 6–8-mo-old *Sle1b*-BAC90 female mice compared with age-matched B6.*Sle1b* females (Fig. 2C). There was a strong inverse correlation between the percentage of GC B cells and the levels of Ly108 and CD84 expression on GC B cells (data not shown). Next, we asked whether the decrease in Spt-GCs in *Sle1b*-BAC90 mice resulted in a decline in the Tfh cell response. B6 and *Sle1b*-BAC90 mice had similar percentages of $CD4^{+}CXCR5^{hi}PD\text{-}1^{hi}$ Tfh cells, $CD4^{+}CD44^{hi}CD62L^{lo}$ short-lived effector/effector memory T cells, and $CD4^{+}CD44^{hi}CD62L^{hi}$ central memory T cells, all of which were significantly lower than in B6.*Sle1b* mice (Fig. 2D, 2E). These data suggest the cooperative function of CD84 and Ly108 in maintaining GC B cell tolerance.

Wild-type CD84 and Ly108 prevent development of ANA-specific AFCs and serum autoantibody titers

Next, we asked whether the reduction in Spt-GC responses in *Sle1b*-BAC90 mice resulted in decreased ANA-specific AFCs and Ab titers. B6 and *Sle1b*-BAC90 mice had significantly lower numbers of dsDNA-, histone-, and nucleosome-specific AFCs in the spleen (Fig. 3A–C), as well as total serum IgM and IgG titers (Fig. 3D, 3E), than did B6.*Sle1b* mice. *Sle1b*-BAC90 mice also exhibited significantly reduced levels of IgG2c-specific Abs against dsDNA, histone, nucleosome (Fig. 3F–H), Sm/RNP, and cardiolipin (Fig. 3J, 3K) as well as IgG2b-specific anti-nucleosome Abs (Fig. 3I) compared with B6.*Sle1b* mice. The reduced autoantibody levels in *Sle1b*-BAC90 mice strongly correlated with the lower percentage of Spt-GC B cells (data not shown).

The cardinal function of GCs is the generation of long-lived AFCs, which primarily reside in BM (19). We asked whether elevated Spt-GC and Tfh cell responses in B6.*Sle1b* mice resulted in more ANA-specific, long-lived BM AFCs and whether the elevated ANA-specific BM AFC response in B6.*Sle1b* mice could be reversed by the introduction of B6 alleles of CD84 and Ly108 in *Sle1b*-BAC90 mice. Although there were significantly higher numbers of ANA-specific AFCs in the BM of B6.*Sle1b* mice, their numbers were markedly reduced in *Sle1b*-BAC90 mice (Fig. 3L–N).

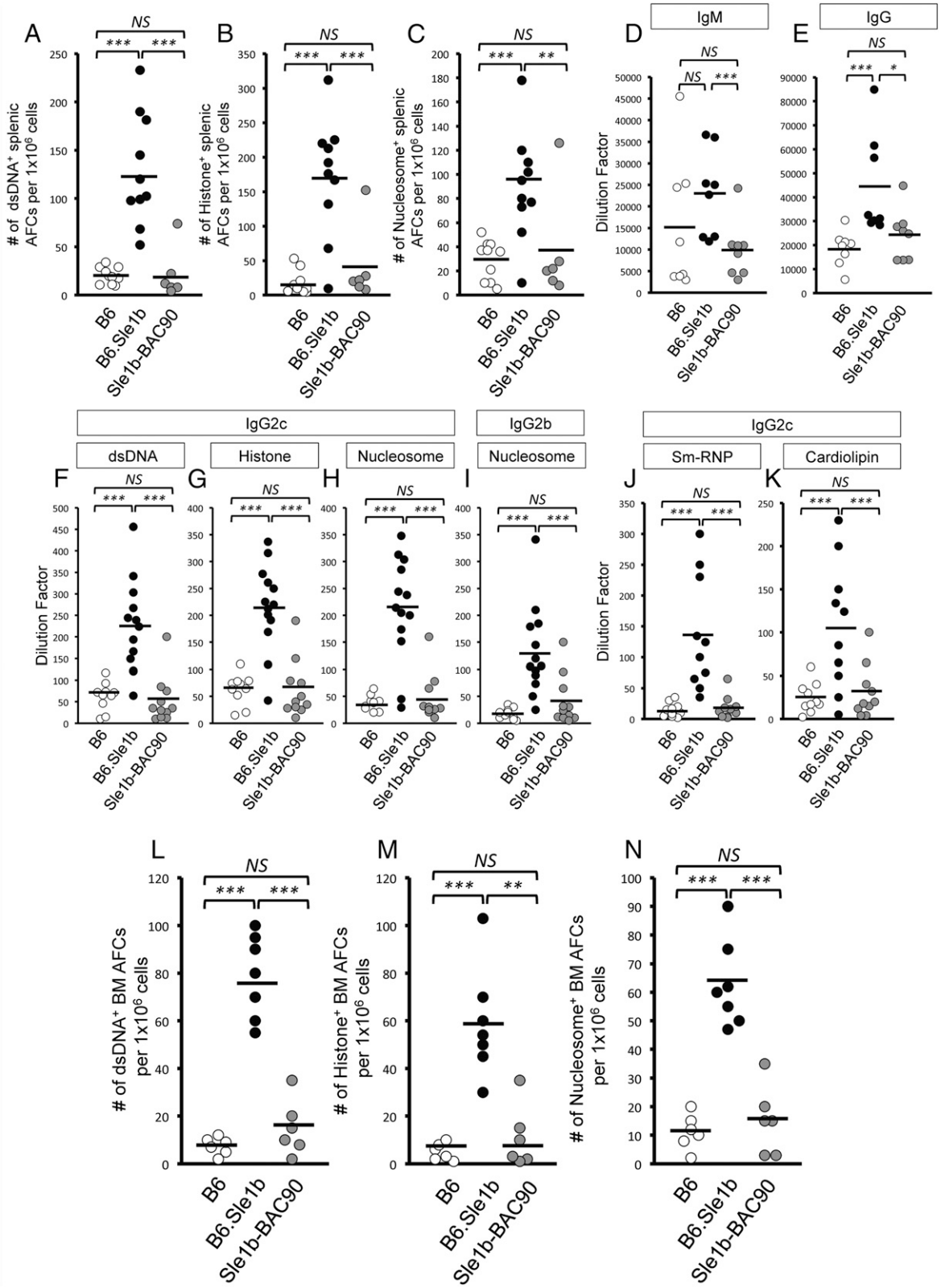

FIGURE 3. Reduction in ANA-specific AFCs and Ab titers in *Sle1b*-BAC90 mice. ELISPOT analysis of dsDNA-specific (**A**), histone-specific (**B**), and nucleosome-specific (**C**) splenic AFCs in 6–8-mo-old B6, B6.*Sle1b*, and *Sle1b*-BAC90 mice. Total IgM (**D**) and IgG (**E**) serum titers at 6–8 mo of age in each group of mice. (**F**–**K**) ELISA analysis of IgG2c-specific Abs against dsDNA, histone, nucleosome, Sm/RNP, and cardiolipin, as well as IgG2b-specific Abs against nucleosome, at 6–8 mo of age. (**L**–**N**) ELISPOT analysis of dsDNA-, histone-, and nucleosome-specific long-lived BM AFCs in 6–8-mo-old mice of the indicated genotypes. Each symbol represents an individual mouse. $*p < 0.05$, $**p < 0.01$, $***p < 0.001$.

The reduction in Spt-GC, Tfh cell, and ANA responses in *Sle1b*-BAC90 mice was not the result of global suppression of the ability of B cells to mount an immune response, because no differences were observed in the foreign Ag–specific GC, Tfh cell, and Ab responses among B6, B6.*Sle1b*, and *Sle1b*-BAC90 mice immunized with SRBCs (data not shown).

*Overexpression of B6-derived CD84 and Ly108 on GC B cells is sufficient to restore tolerance in B6.*Sle1b *mice*

To determine whether the overexpression of B6 alleles of CD84 and Ly108 within GC B cells could restore tolerance, we generated *Sle1b*-BAC90$^{fl/fl}$ mice and crossed them with GC B cell–specific Cg-Ighg1-Cre mice (20, 21). Quantitative PCR analysis of gene copy number and flow cytometric analysis of surface expression confirmed significantly reduced expression levels of the Ly108 and CD84 genes, specifically in GC B cells (Fig. 4A–D) and not in non-GC naive B cells (data not shown), confirming GC B cell–specific deletion of the BAC90 transgene containing B6-CD84 and Ly108 genes in *Sle1b*-BAC90$^{fl/fl}$-Cre mice.

Flow cytometric analysis of 4–5-mo-old *Sle1b*-BAC90$^{fl/fl}$-Cre mice showed increased percentages of GC B cells, Tfh cells, and short-lived effector T cells, as well as increased CD86 expression on B cells, compared with B6 and *Sle1b*-BAC90$^{fl/fl}$ (Cre$^{-/-}$) controls (Fig. 4E–H). These elevated responses in *Sle1b*-BAC90$^{fl/fl}$-Cre mice were similar to the increased responses seen in B6.*Sle1b* mice (Fig. 4E–H). Immunofluorescent staining of spleen sections with GL7, anti-IgD, and anti-CD4 confirmed the flow cytometry data, showing increased numbers and sizes of IgD^{-}GL7^{+} Spt-GCs in B6.*Sle1b* and *Sle1b*-BAC90$^{fl/fl}$-Cre mice compared with B6 and *Sle1b*-BAC90$^{fl/fl}$ controls (Fig. 4I, 4J).

This increase in Spt-GC responses in *Sle1b*-BAC90$^{fl/fl}$-Cre mice resulted in elevated numbers of IgM-, IgG-, dsDNA-, histone-, and nucleosome-specific AFCs in the spleen (Fig. 5A–E), as well as serum IgG2c titers specific for dsDNA, histone, nucleosome, Sm/RNP, and cardiolipin (Fig. 5F–J). Cre-mediated excision of transgenically expressed wild-type Ly108 and CD84 from GC B cells in *Sle1b*-BAC90$^{fl/fl}$-Cre mice resulted in elevated numbers of IgM-, IgG-, dsDNA-, histone-, and nucleosome-specific long-lived AFCs in the BM (Fig. 5K–O), confirming that GC B cell–specific B6 wild-type CD84 and Ly108 expression was sufficient for the restoration of tolerance in B6.*Sle1b* mice.

*Wild-type CD84 and Ly108 expression normalizes BCR signaling, proliferation, and apoptotic capacity of B cells in B6.*Sle1b *mice*

Next, we determined whether elevated Spt-GC responses in B6.*Sle1b* mice compared with B6 controls correlated with increased proliferation of B cells that can potentially drive the autoimmune response. In vitro stimulation of B cells with anti-IgM and anti-CD40 unexpectedly resulted in a reduced number of proliferating B cells at 72 h in B6.*Sle1b* mice compared with B6 controls (Fig. 6A). Moreover, a significantly higher percentage of B cells remained in the G_0/G_1 phase in B6.*Sle1b* mice, resulting in a lower fraction of cells in the S phase compared with B6 controls (Fig. 6B). This reduced proliferation in B6.*Sle1b* mice was corrected in *Sle1b*-BAC90 mice overexpressing B6-CD84 and Ly108 (Fig. 6A, 6B). In line with the lower proliferation rate, stimulation with anti-IgM caused a lower Ca^{2+} flux in B6.*Sle1b* B cells than in B6 B cells (Fig. 6C). Notably, *Sle1b*-BAC90 mice exhibited a Ca^{2+} flux that was similar to B6 mice (Fig. 6C), highlighting a potential cross-talk between BCR and SLAM signaling.

Next, to determine whether the decrease in proliferative capacity of B6.*Sle1b* B cells resulted in increased apoptosis of B6.*Sle1b* B cells, we evaluated B cell survival upon stimulation. In vitro stimulation of B cells with anti-IgM and anti-CD40 resulted in a lower percentage of apoptotic B6.*Sle1b* B cells compared with B6 and *Sle1b*-BAC90 B cells (Fig. 6D). We also determined the percentage of B cells undergoing apoptosis in GCs by measuring the caspase activity in DAPI^{-}B220^{+}Fas^{hi}PNA^{hi} GC B cells. We found a significant decrease in B220^{+}PNA^{hi}Fas^{hi}Caspase^{+} apoptotic GC B cells in B6.*Sle1b* mice compared with B6 controls (Fig. 6E). Overall, the percentage of apoptotic GC B cells in *Sle1b*-BAC90 mice was higher than in B6.*Sle1b* mice, but the difference was not statistically significant (Fig. 6E). We observed no significant difference in the percentage of apoptotic GC B cells between B6 and *Sle1b*-BAC90 mice. Consistent with this finding, staining for apoptotic TUNEL^{+} cells on spleen sections showed fewer apoptotic cells/μm^2 of GC area in B6.*Sle1b* mice than in B6 and *Sle1b*-BAC90 mice (Fig. 6F). Supporting the above findings, our gene-expression analysis revealed significant upregulation of several antiapoptotic genes in B6.*Sle1b* B cells compared with B6 B cells (Table I).

To determine whether there were defects in the BCR signaling pathway in B6.*Sle1b* B cells, we evaluated the phosphorylation status of BCR proximal signaling molecules (BTK and Syk) and downstream molecules (p-38–MAPK and Erk) after BCR activation with anti-IgM using phosphoflow analysis. Consistent with the Ca^{2+} flux results, B6.*Sle1b* B cells exhibited decreased phosphorylation of all of these molecules (Fig. 6G–J). Introduction of the B6 alleles of CD84 and Ly108 in *Sle1b*-BAC90 mice rescued this signaling defect, further supporting the possibility of cross-talk between BCR and SLAM signaling and indicating a role for Ly108 and CD84 in the restoration of peripheral B cell tolerance. Our results also show that B cells from B6.*Sle1b* mice were not anergic and that the reduced signaling activity exhibited by these B cells was not due to primary B cell developmental defects (Supplemental Fig. 4).

Several genes encoding enzymes required for various metabolic pathways, including those involved in cellular energy metabolism, are modulated by the activation of B cells through BCR, CD40L, and TLR ligands (22). Additionally, it was demonstrated that signaling events, which lead to variations in cellular energy metabolism during GC reactions, are necessary for the maintenance and differentiation of GC B cells and plasma cells (21). Given the aforementioned differences in BCR signaling (Fig. 6G–J), we then asked whether B cells from B6, B6.*Sle1b*, and *Sle1b*-BAC90 mice were metabolically different in responding to energy demands upon activation. No significant differences were observed in the baseline oxygen consumption among B cells from B6, B6.*Sle1b*, and *Sle1b*-BAC90 mice following activation with anti-IgM and anti-CD40 (Fig. 6K, 6L). ATP production after exposure to oligomycin also was comparable among these three strains (Fig. 6K, 6L). In addition, B6 and B6.*Sle1b* B cells showed similar maximum respiration, whereas *Sle1b*-BAC90 B cells showed marginally reduced maximal respiration, compared with B6 controls (Fig. 6K, 6L). Notably, B6.*Sle1b* and *Sle1b*-BAC90 B cells had significantly higher glycolysis and glycolytic capacity than did B6 B cells (Fig. 6M, 6N). These results indicate that reduced calcium mobilization and decreased BCR signaling in B6.*Sle1b* B cells did not dampen the energy metabolism in these cells.

Sle1b-*expressing B cells have a lower frequency of conjugate formation with wild-type T cells, which is reversed by the overexpression of wild-type CD84 and Ly108*

Previous studies showed that SAP expression in T cells is required for effective B and T cell conjugation leading to optimal GC responses during T cell–dependent antigenic stimulation or viral infection (23, 24). The effect of B cell–intrinsic expression of lupus-associated SLAM family receptors on conjugate formation in the context of autoimmunity is not clear. We asked whether polymorphic SLAM expression in B cells from B6.*Sle1b* mice led to differential interaction with T cells, affecting their ability to form B cell–T cell conjugates. We further asked whether overexpression of B6-derived CD84 and Ly108 in B6.*Sle1b* B cells could normalize such potential differences in the ability of B6.*Sle1b* B cells to form conjugates with T cells.

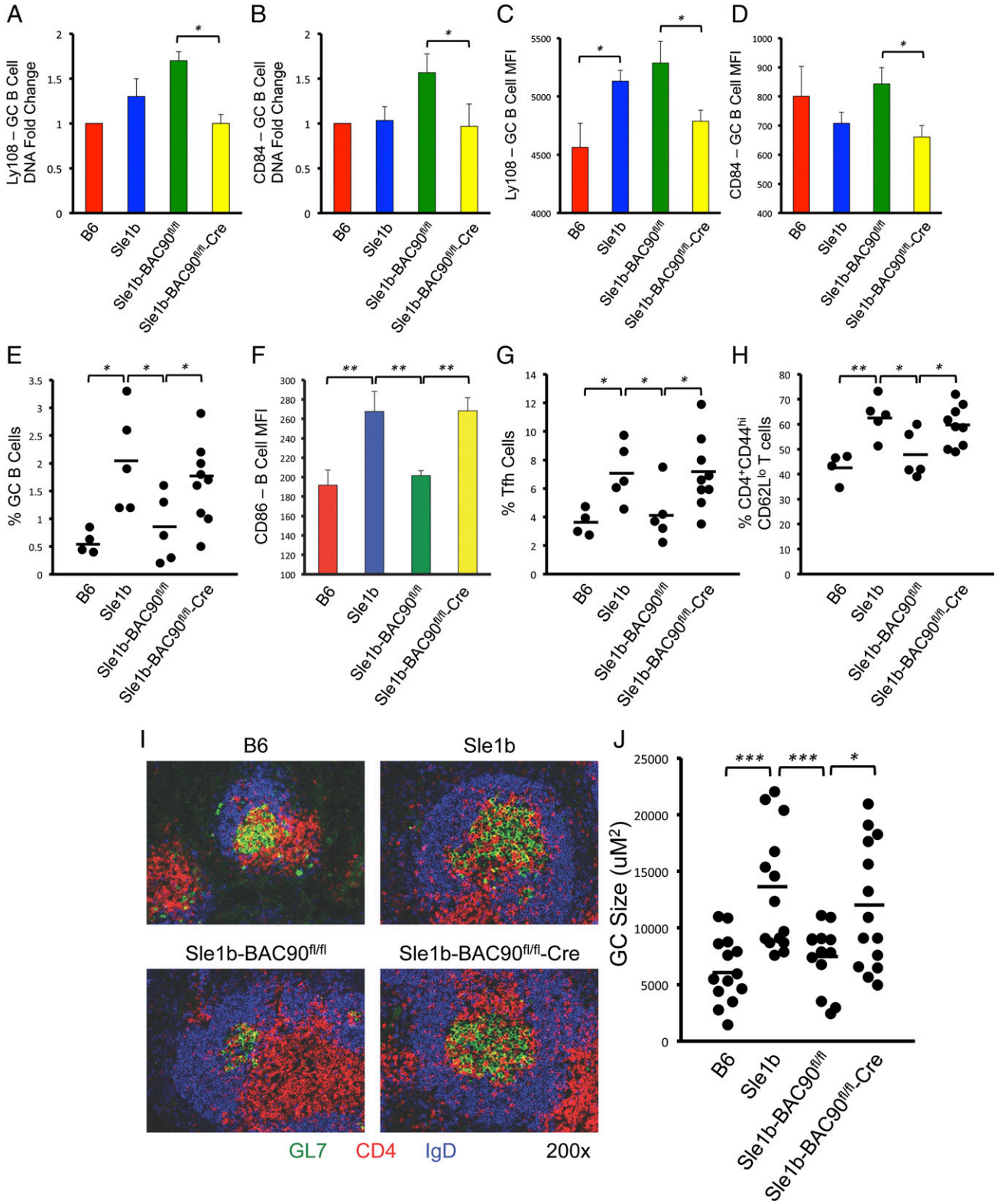

FIGURE 4. GC B cell–intrinsic effect of overexpression of B6 Ly108 and CD84 on restoration of tolerance. (**A** and **B**) GC B cells were sorted (FACSAria) and analyzed for genomic expression of Ly108 and CD84, which were normalized to B6 control. (**C** and **D**) Flow cytometric analysis of Ly108 and CD84 expression levels (MFI) on GC B cells. (**E**) Scatter plots showing the percentages of GC B cells. (**F**) MFI of CD86 levels on B cells. Scatter plots showing the percentages of Tfh cells (**G**) and short-lived effector/effector memory T cells (**H**) in 4–5-mo-old mice. (**I**) Representative images of spleen sections from 4–5-mo-old mice stained with GL-7 (green), anti-CD4 (red), and anti-IgD (blue). These data represent three to five randomly picked mice/group. (**J**) Scatter plot showing GC sizes for each group of mice at 4–5 mo of age. $*p < 0.05$, $**p < 0.01$, $***p < 0.001$.

We used an in vitro flow cytometry–based B and T cell conjugation assay in which purified B cells from B6, B6.*Sle1b*, and *Sle1b*-BAC90 mice were activated with anti-IgM and LPS and loaded with OVA peptide to present to B6 OT-II–transgenic T cells specific for $OVA_{323–339}$. B6.*Sle1b* B cells formed a significantly reduced number of conjugates over the course of 60 min compared

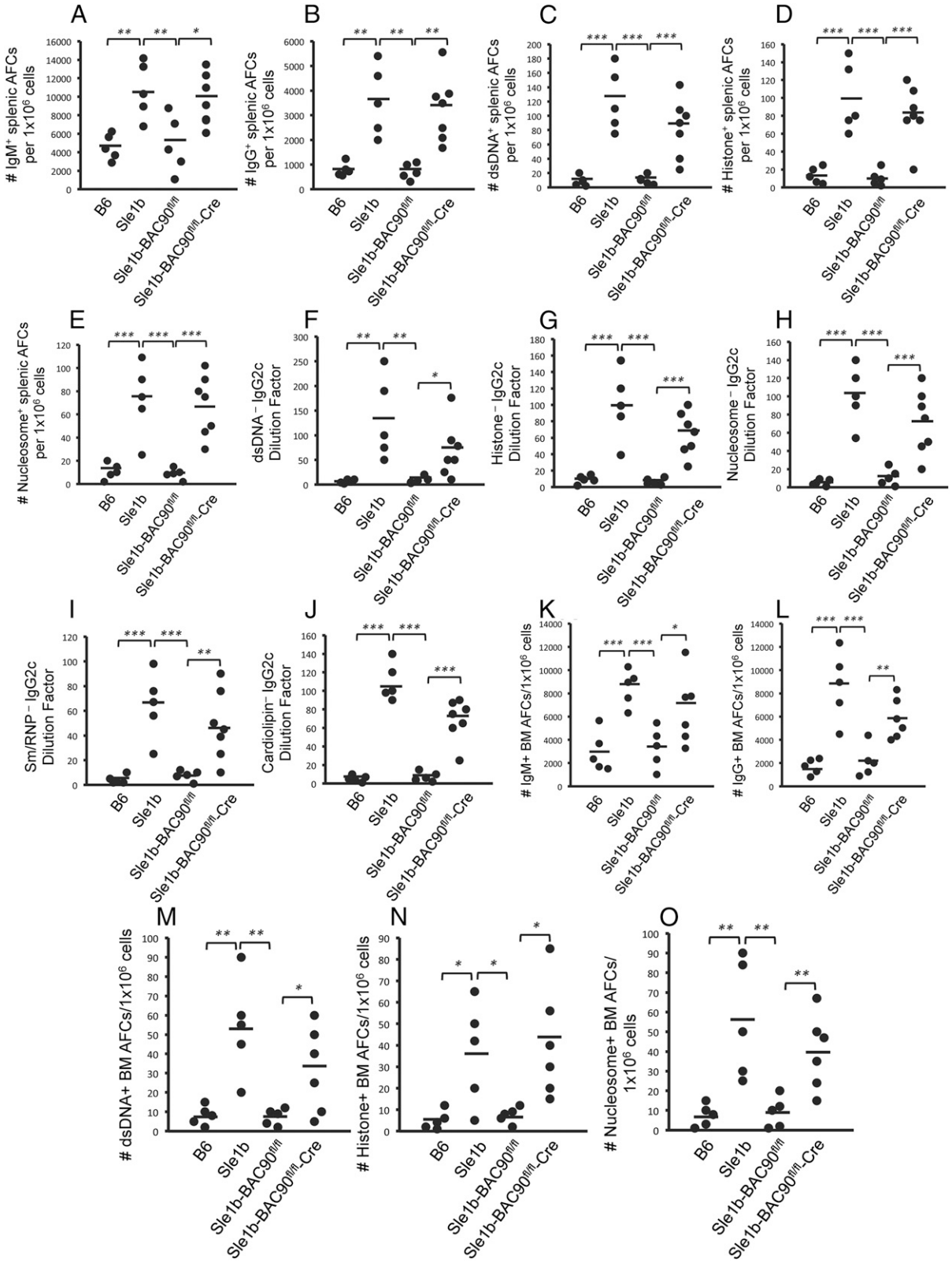

FIGURE 5. GC B cell–specific excision of B6 Ly108 and CD84 in *Sle1b*-BAC90 mice reinstates loss of tolerance to ANA. (**A**–**E**) ELISPOT analysis of IgM-, IgG-, dsDNA-, histone-, and nucleosome-specific splenic AFCs in 4–5-mo-old mice. (**F**–**J**) IgG2c-specific Abs against dsDNA, histone, nucleosome, Sm/RNP, and cardiolipin, as well as IgG2b-specific Abs against nucleosome, were measured using ELISA. (**K**–**O**) ELISPOT analysis of IgM-, IgG-, dsDNA-, histone-, and nucleosome-specific long-lived BM AFCs at 4–5 mo. Each symbol represents an individual mouse. $*p < 0.05$, $**p < 0.01$, $***p < 0.001$.

with B cells from B6 mice; this was corrected when B cells were from *Sle1b*-BAC90 mice (Fig. 7A).

To track B cell–T cell interactions in real time, 2D confocal images of conjugates between activated B cells and OT-II T cells were acquired sequentially every 30 s for 60 min (Fig. 7B, 7C). Consistent with the flow cytometry data, the percentage of B cell–OT-II T cell conjugates was significantly lower over time when B cells were from B6.*Sle1b* mice compared with B6 or *Sle1b*-BAC90

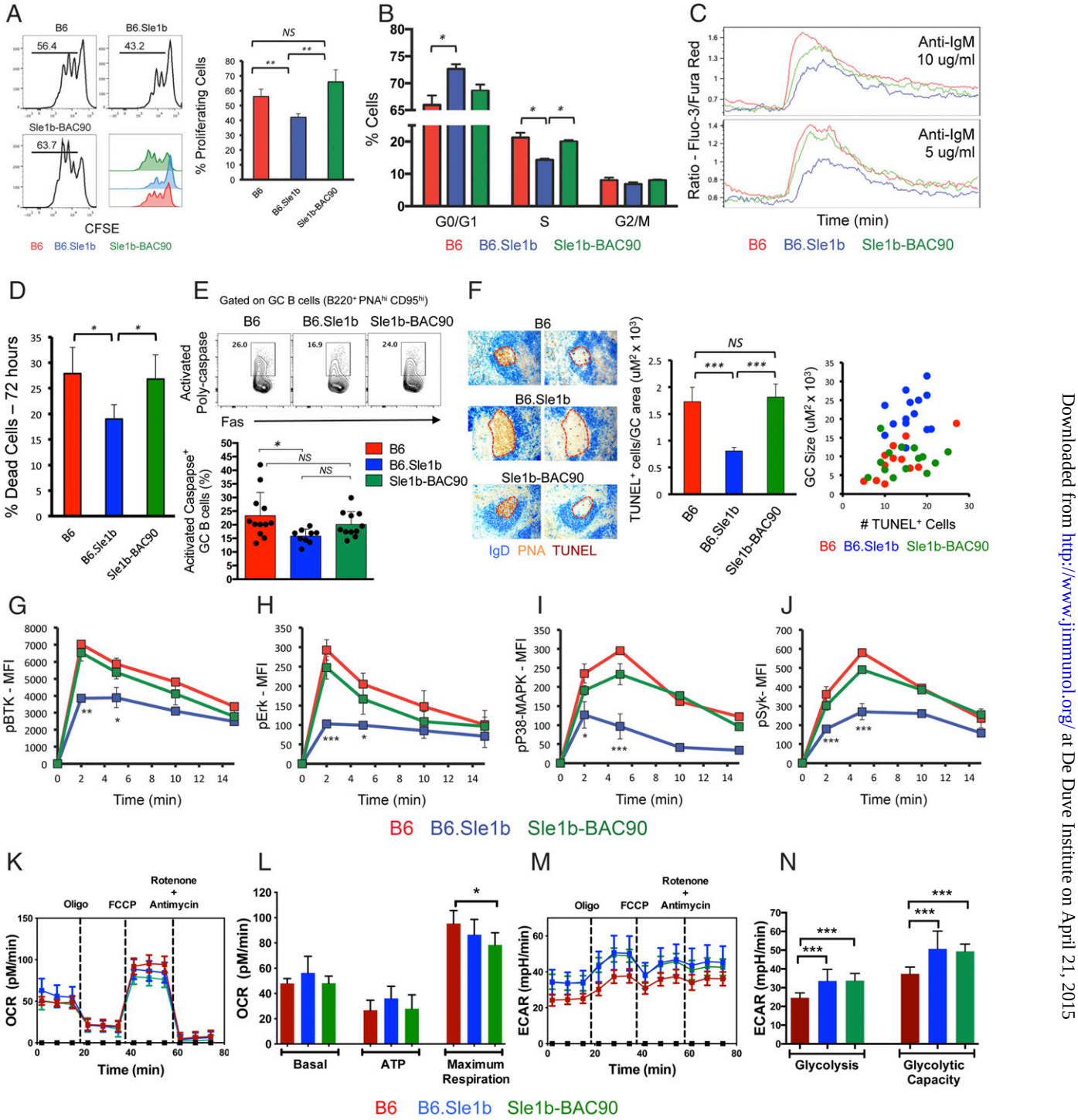

FIGURE 6. Analysis of B cell proliferation, apoptosis, signaling, and cellular metabolism. (**A**) In vitro proliferation of CFSE-labeled B cells stimulated with anti-IgM and anti-CD40 (*left panel*). Bar graph of the percentages of proliferating B cells (*right panel*). (**B**) Cell cycle analysis of purified B cells after anti-IgM and anti-CD40 stimulation by PI staining. (**C**) Calcium flux of B cells after anti-IgM stimulation. (**D**) Bar graph of the percentages of dead cells after anti-IgM and anti-CD40 stimulation. (**E**) Contour plots show the representative gating strategy for GC B cells stained ex vivo with SR-VAD-FMK, a Poly Caspase probe (*upper panel*). Bar graph shows the percentage of GC B cells positive for activated poly caspases in the indicated strains (*lower panel*). Each symbol represents an individual mouse. Data are mean and SD. (**F**) Consecutive spleen sections were stained for IgD (blue), PNA (red), and TUNEL (brown) (*left panel*). Original magnification ×100. Data are representative of five mice/group. Bar graph depicting the ratio of TUNEL$^+$ cells and GC size ($\mu m^2 \times 10^3$) (*middle panel*). Correlation between the number of TUNEL$^+$ cells and the GC size (*right panel*). (**G**–**J**) Flow cytometric analysis to evaluate the kinetics of phosphorylation of BtK, Erk, p38/MAPK, and Syk after anti-IgM stimulation of B cells. Representative plots of OCR (**K**) and ECAR (**M**) in B6, B6.*Sle1b*, and *Sle1b*-BAC90 B cells stimulated with anti-IgM and anti-CD40 for 18 h. (**L**) Bar graph of average basal oxygen consumption; ATP production through ATP synthase and the maximal electron transport capacity of activated B cells from three or four mice/group. (**N**) Bar graph of average ECAR values for glycolysis and the glycolytic capacity of activated B cells from three or four mice/strain. *$p \leq 0.05$, **$p \leq 0.01$, ***$p \leq 0.001$.

mice (Fig. 7D, *left panel*). We also measured the duration of contacts between OT-II T cells and B cells from each strain over a 60-min period. We found similar B cell–T cell contact duration time between B cells from B6 and B6.*Sle1b* mice. The contact

Table I. List of antiapoptotic genes upregulated in B cells from B6.*Sle1b* mice

Gene Name	Fold Change	*p* Value
BCL2L1	2.2	0.03
SPHK1	2.2	0.007
HMGB2	2.5	0.048
BIRC5	2.6	0.011
RRM2	1.9	0.018
METAP2	1.6	0.031

These antiapoptotic genes were significantly upregulated in sorted B cells derived from 3-mo-old B6.*Sle1b* mice, as determined by Illumina Bead Chip arrays (Mouse WG-6 V2). Gene expression is shown in terms of increased fold change in B6.*Sle1b* mice compared with B6 controls. Statistical analysis was performed using the pairwise homogeneous *t* test.

duration time was higher with B cells from *Sle1b*-BAC90 mice compared with B6 and B6.*Sle1b* mice (Fig. 7D, *right panel*).

Phosphoflow analysis of B cells after conjugate formation with OT-II T cells showed similar phosphorylation levels of BTK and p38-MAPK among all three strains (Fig. 7E, 7H) but reduced phosphorylation of Erk and Syk in B cells from B6.*Sle1b* mice compared with B6 and *Sle1b*-BAC90 mice (Fig. 7F, 7G). These data suggest that differential expression of CD84 and Ly108 on B cells could alter B and T cell interactions, resulting in reduced BCR signaling. It is plausible that such variations in the frequency of B and T cell interactions and lower BCR signaling might allow autoimmune B cells to escape the GC tolerance checkpoint.

Discussion

Polymorphisms in SLAM family genes are implicated in both murine and human lupus (1, 2, 17, 25–27). Using B6.*Sle1b* mice that express the NZM2410/NZW lupus strain–derived SLAM family genes, we showed previously that this sublocus alters B cell tolerance at the GC checkpoint, leading to increased ANA-specific AFCs and ANA titers (3, 16). However, the mechanisms by which B cell–intrinsic expression of polymorphic SLAM family genes may alter B cell tolerance at the GC checkpoint and the SLAM family members required for mediating this process were not

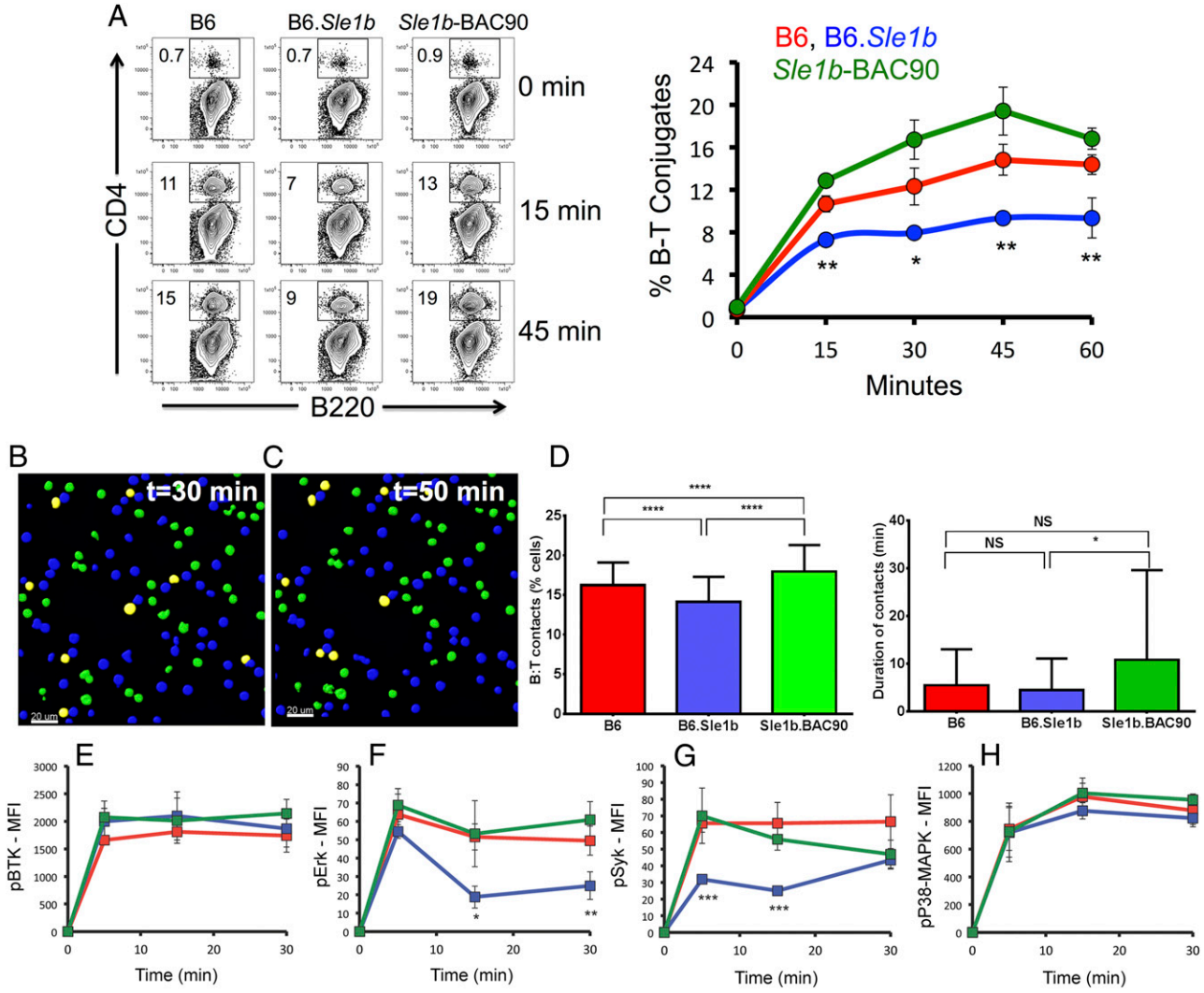

FIGURE 7. Reduced B cell–T cell conjugate formation in B6.*Sle1b* mice. (**A**) Representative flow cytometry plots of $B220^+$ B cell and $CD4^+$ OT-II T cell conjugate formation (*left panel*). Conjugate formation was calculated as $B220^+CD4^+$ double positive for each mouse group over the course of 60 min. Line graph of the kinetics of B cell–T cell conjugate formation (*right panel*). Representative 2D confocal images of B6 B cells (blue) and OT-II T cells (green) in coculture at 30 min (**B**) and 50 min (**C**). The B and T cells in contact with each other are shown in yellow. Scale bars, 20 μm. (**D**) Average percentage (*left panel*) and duration (*right panel*) of contacts between OT-II T cells and B cells from the indicated strains over a 60-min period. The analysis was performed twice, with B cells pooled from two or three mice/group. (**E**–**H**) Kinetics of phosphorylation of BtK, Erk, p38/MAPK, and Syk in B cells during conjugate formation with T cells over the course of 30 min. $*p < 0.05$, $**p < 0.01$, $***p < 0.001$, $****p < 0.0001$.

addressed. In this study, by analyzing seven B6.*Sle1b* mouse lines carrying various BAC transgenes of B6 alleles of SLAM and non-SLAM family genes spanning the entire *Sle1b* locus, we identified that Ly108 and CD84 play essential roles in the loss of B cell tolerance in B6.*Sle1b* mice. Overexpression of B6 wild-type CD84 and Ly108 can restore B cell tolerance at the GC checkpoint, leading to reduced numbers of ANA-specific long-lived AFCs in BM. Subsequently, taking advantage of GC B cell–specific Cre mice in which Cre conditionally removed transgenically expressed B6 alleles of CD84 and Ly108 on GC B cells, we further demonstrate that the expression of polymorphic CD84 and Ly108 on GC B cells is critical for the loss of tolerance to nuclear Ags in B6.*Sle1b* mice. These results highlight the importance of CD84 and Ly108 expression on GC B cells in regulating Spt-GC and Tfh cell responses and in preventing autoimmunity.

Our in vitro functional assays revealed lower Ca^{2+} flux, reduced proliferation, and apoptosis of B cells expressing *Sle1b* compared with B6, all of which were restored in *Sle1b*-BAC90 mice overexpressing B6 alleles of CD84 and Ly108. Consistent with these data, we found reduced levels of phosphorylation of several molecules in the BCR signaling pathway in B cells from B6.*Sle1b* mice, whereas B6 and *Sle1b*-BAC90 mice showed comparable levels of phosphorylation of these molecules. Our results are consistent with a previous report (4) showing lower Ca^{2+} flux and less cell death of hen egg lysozyme (HEL)-transgenic B cells expressing *Sle1b* (*Sle1b*-HEL transgenic) upon BCR stimulation. However, Kumar et al. (4) reported increased proliferation of *Sle1b*-HEL–transgenic B cells, whereas we found a modest reduction in the proliferation of B cells expressing *Sle1b*. This discrepancy in the proliferation of *Sle1b* B cells may have resulted from the difference in Ag specificity (i.e., HEL transgenic versus polyreactive).

The mechanism by which autoreactive B cells in B6.*Sle1b* mice are selected into autoantibody-producing long-lived AFCs or memory B cells is not clear. Based on our data showing reduced proliferation and apoptosis of B cells expressing *Sle1b* and the reversal of these phenotypes with overexpression of B6-derived CD84 and Ly108, we suggest that the increased spontaneous GC, Tfh cell, and long-lived AFC responses in B6.*Sle1b* mice may not be the result of an enhanced positive selection of autoreactive B cells in GCs. Rather, we believe that autoreactive B cell development in GCs of B6.*Sle1b* mice is due to altered negative selection of GC B cells. We propose two plausible mechanisms by which polymorphic SLAM expression in B cells from B6.*Sle1b* mice may help autoreactive B cells escape negative selection in GCs. One mechanism is that polymorphic SLAM expression in B6.*Sle1b* B cells helps to reduce BCR signaling upon engagement of self-Ags, which allows these cells to survive in the GC and not undergo negative selection.

We propose a second scenario whereby GC B cells interact with T cells. Given the increased frequency of Tfh cells in B6.*Sle1b* mice, the chances of B cell–T cell interactions in GCs are very high. Therefore, given our data from the conjugate assay, we suggest that reduced B cell–T cell conjugates, resulting from B cell–intrinsic expression of polymorphic SLAMs, helps to maintain reduced BCR signaling in B cells expressing *Sle1b*. On one hand, this differential frequency of interaction of B6.*Sle1b* B cells with T cells may help autoreactive B cells to escape negative selection in GCs by reducing BCR signaling; on the other hand, it provides sufficient survival signals to these B cells to proliferate (albeit at a slower rate than B6 controls) and differentiate into autoantibody-producing AFCs. Consistent with this idea, we previously observed augmented GC responses of DNA and p-azophenylarsonate dual-reactive B cells from Ig V_H knock-in mice (named HKIR) expressing *Sle1b* (16). Under non-autoimmune conditions, because of their DNA reactivity, HKIR p-azophenylarsonate–DNA dual-reactive B cells are negatively regulated in GCs, presumably by the GC tolerance checkpoint (28–30). However, autoimmune susceptibility, as in B6.*Sle1b* mice, alters their negative selection in GCs (16). Recently, Sinai et al. (31) also reported that altered B and T cell interactions were responsible for an increased GC B cell phenotype in vitro in autoimmune-prone B6.*Sle1b* mice.

Anergic B cells have arrested development, are excluded from B cell follicles, and are unable to mobilize calcium (32). Anergic B cells are also unable to proliferate, upregulate activation markers, mediate BCR signaling, or mount an immune response after BCR engagement (32). Our results show that B6.*Sle1b* B cells exhibit normal B cell development in the BM and spleen, are present in B cell follicles, and seed GCs; thus, they do not exhibit an anergic state. Analysis of the cellular energy metabolism also indicates that reduced calcium mobilization and lower BCR signaling upon stimulation of B6.*Sle1b* B cells do not dampen the energy metabolism in these cells. B6.*Sle1b* B cells appear to be comparable, if not better, in responding to the high-energy demands upon activation. In a recent comparative analysis, Rathmell and colleagues (33) found that anergic B cells were metabolically suppressed, whereas B cells from autoimmune BAFF-transgenic mice were metabolically more active with increased glycolytic efficiency, which was necessary for autoantibody production. This study is in line with our data showing that B6.*Sle1b* B cells are not anergic; rather, they can undergo optimal metabolic reprogramming upon activation to produce high titers of autoantibodies.

The functional and mechanistic roles of Ly108 and CD84 in the context of GCs are unclear. Ly108 was proposed to act as a molecular rheostat that determines the stringency with which autoreactive B cells are purged during primary development (4), whereas other studies suggested similar functions for Ly108 in T cells (5, 34). Although our data indicate that polymorphisms in CD84 and Ly108 in B cells determine the efficiency of tolerance, we cannot exclude a possible contribution of Ly108 expression by T cells, particularly with respect to the production of IFN-γ (35). IFN-γ was demonstrated to drive pathogenic accumulation of Tfh cells in *Roquin*^{san} mice and promote Ab class switching to pathogenic IgG2c, both of which are observed in B6.*Sle1b* mice (36–38).

Although CD84 and Ly108 were demonstrated to be integral for optimal GC responses against protein immunization (23), no such defect was observed in mice deficient in CD84 in the context of an acute lymphocytic choriomeningitis virus or vaccinia virus infection (24). Our analysis also revealed no defect in spontaneous or SRBC-induced GC and Tfh cell responses in mice deficient in either CD84 or Ly108 (data not shown). These data indicate redundancy in functions of SLAM family receptors; however, these earlier studies did not investigate the B cell–intrinsic expression of polymorphic CD84 and Ly108 in the Spt-GC response. Our data suggest that CD84 and Ly108 function in a regulatory capacity in B cells, because Spt-GC responses correlated inversely with CD84 and Ly108 expression, specifically on GC B cells (data not shown). In addition, in vitro stimulation with anti-Ly108 resulted in increased CD84 levels on activated B6 B cells, which was defective in *Sle1b* B cells but mostly restored in *Sle1b*-BAC90 B cells (data not shown), indicating that the functions of these two SLAM family genes may be tightly linked. These data suggest that altered signaling in B cells mediated by *Sle1b*-derived CD84 and Ly108 may lead to a modulation in B and T cell interactions and subsequent selection in GCs. Consistent with this idea, we observed impaired B and T cell conjugation when B cells expressed *Sle1b*, which was restored by B cell expression of wild-type CD84 and Ly108.

Earlier studies focused on SLAM signaling in T cells and NKT cells owing to the discovery of the SAP molecule, which is highly expressed in these cell types (2). SAP regulates T cell–mediated help (39), Tfh cell development (40), cytokine production (41), and GC response (42). SAP expression in T cells, but not in B cells, is required for a humoral immune response (43). Ly108 also was shown to regulate T cell signaling via the SAP–Fyn pathway (34). Crotty and colleagues (24) further suggested that Ly108 regulates T cell and B cell interactions by modulating the ratio of positive/negative signals mediated by SAP and SHP-1. The requirement for SAP and T cells in autoimmune responses also was described in lupus-prone MRL-FAS^{lpr} (44), Sanroque (45), and B6.*Sle1b* mice (46).

Although previous studies highlighted the importance of SLAM–SAP signaling within T cells in shaping T cell–mediated B cell responses, whether similar signaling mechanism exists in B cells has not been defined previously. Detre et al. (47) recently reported the role of SAP in modulating B cell functions. Because B cells do not express SAP, the mechanism by which SAP deficiency alters the B cell response is not clear. We observed no differences in SAP transcript levels in T and B cells (including Tfh cells and GC B cells) among B6, B6.*Sle1b*, and *Sle1b*-BAC90 mice. A recent study implicated the role of SAP-related molecule EAT-2 in mediating its effects in NK cells by linking SLAM family receptors to phospholipase Cγ, calcium flux, and Erk kinase (48). Whether signaling through this or other unknown adaptor molecules is compromised in B6.*Sle1b* B cells, resulting in lower calcium flux and reduced Erk phosphorylation, remains to be determined.

In summary, we showed that CD84 and Ly108 expression on GC B cells is critical for maintaining peripheral B cell tolerance at the GC checkpoint. Our data further highlight the importance of the GC pathway in autoimmune disease pathogenesis and suggest that GC B cell–specific CD84 and Ly108 may be therapeutic targets for systemic lupus erythematosus.

Acknowledgments

We thank Drs. Aron Lukacher, Tim Manser, and Milena Bogunovic for critical reading of the manuscript and helpful discussions. We thank Stephanie Schell for proofreading the manuscript. Finally, we thank Dr. Jose Casco (the University of Texas Southwestern Medical Center) for maintenance and transfer of BAC-transgenic mice and the Penn State Hershey flow cytometry core facility for their service.

Disclosures

The authors have no financial conflicts of interest.

References

1. Wang, A., F. Batteux, and E. K. Wakeland. 2010. The role of SLAM/CD2 polymorphisms in systemic autoimmunity. *Curr. Opin. Immunol.* 22: 706–714.
2. Cannons, J. L., S. G. Tangye, and P. L. Schwartzberg. 2011. SLAM family receptors and SAP adaptors in immunity. *Annu. Rev. Immunol.* 29: 665–705.
3. Wandstrat, A. E., C. Nguyen, N. Limaye, A. Y. Chan, S. Subramanian, X.-H. Tian Y.-S. Yim, A. Pertsemlidis, H. R. Garner, Jr., L. Morel, and E. K. Wakeland. 2004. Association of extensive polymorphisms in the SLAM/CD2 gene cluster with murine lupus. *Immunity* 21: 769–780.
4. Kumar, K. R., L. Li, M. Yan, M. Bhaskarabhatla, A. B. Mobley, C. Nguyen, J. M. Mooney, J. D. Schatzle, E. K. Wakeland, and C. Mohan. 2006. Regulation of B cell tolerance by the lupus susceptibility gene Ly108. *Science* 312: 1665–1669.
5. Keszei, M., C. Detre, S. T. Rietdijk, P. Muñoz, X. Romero, S. B. Berger, S. Calpe, G. Liao, W. Castro, A. Julien, et al. 2011. A novel isoform of the Ly108 gene ameliorates murine lupus. *J. Exp. Med.* 208: 811–822.
6. Koh, A. E., S. W. Njoroge, M. Feliu, A. Cook, M. K. Selig, Y. E. Latchman, A. H. Sharpe, R. B. Colvin, and E. Paul. 2011. The SLAM family member CD48 (Slamf2) protects lupus-prone mice from autoimmune nephritis. *J. Autoimmun.* 37: 48–57.
7. Keszei, M., Y. E. Latchman, V. K. Vanguri, D. R. Brown, C. Detre, M. Morra, C. V. Arancibia-Carcamo, E. Paul, S. Calpe, W. Castro, et al. 2011. Autoantibody production and glomerulonephritis in congenic Slamf1$^{-/-}$ and Slamf2$^{-/-}$ [B6.129] but not in Slamf1$^{-/-}$ and Slamf2$^{-/-}$ [BALB/c.129] mice. *Int. Immunol.* 23: 149–158.
8. de Salort, J., M. Cuenca, C. Terhorst, P. Engel, and X. Romero. 2013. Ly9 (CD229) Cell-Surface Receptor is Crucial for the Development of Spontaneous Autoantibody Production to Nuclear Antigens. *Front. Immunol.* 4: 225.
9. Cappione, A., III, J. H. Anolik, A. Pugh-Bernard, J. Barnard, P. Dutcher, G. Silverman, and I. Sanz. 2005. Germinal center exclusion of autoreactive B cells is defective in human systemic lupus erythematosus. *J. Clin. Invest.* 115: 3205–3216.
10. Vinuesa, C. G., I. Sanz, and M. C. Cook. 2009. Dysregulation of germinal centres in autoimmune disease. *Nat. Rev. Immunol.* 9: 845–857.
11. Luzina, I. G., S. P. Atamas, C. E. Storrer, L. C. daSilva, G. Kelsoe, J. C. Papadimitriou, and B. S. Handwerger. 2001. Spontaneous formation of germinal centers in autoimmune mice. *J. Leukoc. Biol.* 70: 578–584.
12. Bygrave, A. E., K. L. Rose, J. Cortes-Hernandez, J. Warren, R. J. Rigby, H. T. Cook, M. J. Walport, T. J. Vyse, and M. Botto. 2004. Spontaneous autoimmunity in 129 and C57BL/6 mice-implications for autoimmunity described in gene-targeted mice. *PLoS Biol.* 2: E243.
13. Carlucci, F., J. Cortes-Hernandez, L. Fossati-Jimack, A. E. Bygrave, M. J. Walport, T. J. Vyse, H. T. Cook, and M. Botto. 2007. Genetic dissection of spontaneous autoimmunity driven by 129-derived chromosome 1 Loci when expressed on C57BL/6 mice. *J. Immunol.* 178: 2352–2360.
14. Morel, L., K. R. Blenman, B. P. Croker, and E. K. Wakeland. 2001. The major murine systemic lupus erythematosus susceptibility locus, Sle1, is a cluster of functionally related genes. *Proc. Natl. Acad. Sci. USA* 98: 1787–1792.
15. Rahman, Z. S., S. P. Rao, S. L. Kalled, and T. Manser. 2003. Normal induction but attenuated progression of germinal center responses in BAFF and BAFF-R signaling-deficient mice. *J. Exp. Med.* 198: 1157–1169.
16. Wong, E. B., T. N. Khan, C. Mohan, and Z. S. M. Rahman. 2012. The lupus-prone NZM2410/NZW strain-derived Sle1b sublocus alters the germinal center checkpoint in female mice in a B cell-intrinsic manner. *J. Immunol.* 189: 5667–5681.
17. Cunninghame Graham, D. S., T. J. Vyse, P. R. Fortin, A. Montpetit, Y.-C. Cai, S. Lim, T. McKenzie, L. Farwell, B. Rhodes, L. Chad, et al; CaNIOS GenES Investigators. 2008. Association of LY9 in UK and Canadian SLE families. *Genes Immun.* 9: 93–102.
18. Jørgensen, T. N., J. Alfaro, H. L. Enriquez, C. Jiang, W. M. Loo, S. Atencio, M. R. G. Bupp, C. M. Mailloux, T. Metzger, S. Flannery, et al. 2010. Development of murine lupus involves the combined genetic contribution of the SLAM and FcgammaR intervals within the Nba2 autoimmune susceptibility locus. *J. Immunol.* 184: 775–786.
19. Chu, V. T., and C. Berek. 2013. The establishment of the plasma cell survival niche in the bone marrow. *Immunol. Rev.* 251: 177–188.
20. Casola, S., G. Cattoretti, N. Uyttersprot, S. B. Koralov, J. Seagal, Z. Hao, A. Waisman, A. Egert, D. Ghitza, and K. Rajewsky. 2006. Tracking germinal center B cells expressing germ-line immunoglobulin gamma1 transcripts by conditional gene targeting. *Proc. Natl. Acad. Sci. USA* 103: 7396–7401.
21. Heise, N., N. S. De Silva, K. Silva, A. Carette, G. Simonetti, M. Pasparakis, and U. Klein. 2014. Germinal center B cell maintenance and differentiation are controlled by distinct NF-κB transcription factor subunits. *J. Exp. Med.* 211: 2103–2118.
22. Zhu, X., R. Hart, M. S. Chang, J.-W. Kim, S. Y. Lee, Y. A. Cao, D. Mock, E. Ke, B. Saunders, A. Alexander, et al. 2004. Analysis of the major patterns of B cell gene expression changes in response to short-term stimulation with 33 single ligands. *J. Immunol.* 173: 7141–7149.
23. Cannons, J. L., H. Qi, K. T. Lu, M. Dutta, J. Gomez-Rodriguez, J. Cheng, E. K. Wakeland, R. N. Germain, and P. L. Schwartzberg. 2010. Optimal germinal center responses require a multistage T cell:B cell adhesion process involving integrins, SLAM-associated protein, and CD84. *Immunity* 32: 253–265.
24. Kageyama, R., J. L. Cannons, F. Zhao, I. Yusuf, C. Lao, M. Locci, P. L. Schwartzberg, and S. Crotty. 2012. The receptor Ly108 functions as a SAP adaptor-dependent on-off switch for T cell help to B cells and NKT cell development. *Immunity* 36: 986–1002.
25. Chatterjee, M., C. M. Hedrich, T. Rauen, C. Ioannidis, C. Terhorst, and G. C. Tsokos. 2012. CD3-T cell receptor co-stimulation through SLAMF3 and SLAMF6 receptors enhances RORγt recruitment to the IL17A promoter in human T lymphocytes. *J. Biol. Chem.* 287: 38168–38177.
26. Chatterjee, M., T. Rauen, K. Kis-Toth, V. C. Kyttaris, C. M. Hedrich, C. Terhorst, and G. C. Tsokos. 2012. Increased expression of SLAM receptors SLAMF3 and SLAMF6 in systemic lupus erythematosus T lymphocytes promotes Th17 differentiation. *J. Immunol.* 188: 1206–1212.
27. Chatterjee, M., K. Kis-Toth, T.-H. Thai, C. Terhorst, and G. C. Tsokos. 2011. SLAMF6-driven co-stimulation of human peripheral T cells is defective in SLE T cells. *Autoimmunity* 44: 211–218.
28. Notidis, E., L. Heltemes, and T. Manser. 2002. Dominant, hierarchical induction of peripheral tolerance during foreign antigen-driven B cell development. *Immunity* 17: 317–327.
29. Heltemes-Harris, L., X. Liu, and T. Manser. 2004. Progressive surface B cell antigen receptor down-regulation accompanies efficient development of antinuclear antigen B cells to mature, follicular phenotype. *J. Immunol.* 172: 823–833.
30. Rahman, Z. S., B. Alabyev, and T. Manser. 2007. FcgammaRIIB regulates autoreactive primary antibody-forming cell, but not germinal center B cell, activity. *J. Immunol.* 178: 897–907.
31. Sinai, P., I. M. Dozmorov, R. Song, P. L. Schwartzberg, E. K. Wakeland, and C. Wülfing. 2014. T/B-cell interactions are more transient in response to weak stimuli in SLE-prone mice. *Eur. J. Immunol.* 44: 3522–3531.

32. Cambier, J. C., S. B. Gauld, K. T. Merrell, and B. J. Vilen. 2007. B-cell anergy: from transgenic models to naturally occurring anergic B cells? *Nat. Rev. Immunol.* 7: 633–643.
33. Caro-Maldonado, A., R. Wang, A. G. Nichols, M. Kuraoka, S. Milasta, L. D. Sun, A. L. Gavin, E. D. Abel, G. Kelsoe, D. R. Green, and J. C. Rathmell. 2014. Metabolic reprogramming is required for antibody production that is suppressed in anergic but exaggerated in chronically BAFF-exposed B cells. *J. Immunol.* 192: 3626–3636.
34. Zhong, M.-C., and A. Veillette. 2008. Control of T lymphocyte signaling by Ly108, a signaling lymphocytic activation molecule family receptor implicated in autoimmunity. *J. Biol. Chem.* 283: 19255–19264.
35. Howie, D., S. Okamoto, S. Rietdijk, K. Clarke, N. Wang, C. Gullo, J. P. Bruggeman, S. Manning, A. J. Coyle, E. Greenfield, et al. 2002. The role of SAP in murine CD150 (SLAM)-mediated T-cell proliferation and interferon gamma production. *Blood* 100: 2899–2907.
36. Peng, S. L., S. J. Szabo, and L. H. Glimcher. 2002. T-bet regulates IgG class switching and pathogenic autoantibody production. *Proc. Natl. Acad. Sci. USA* 99: 5545–5550.
37. Baudino, L., S. Azeredo da Silveira, M. Nakata, and S. Izui. 2006. Molecular and cellular basis for pathogenicity of autoantibodies: lessons from murine monoclonal autoantibodies. *Springer Semin. Immunopathol.* 28: 175–184.
38. Lee, S. K., D. G. Silva, J. L. Martin, A. Pratama, X. Hu, P.-P. Chang, G. Walters, and C. G. Vinuesa. 2012. Interferon-γ excess leads to pathogenic accumulation of follicular helper T cells and germinal centers. *Immunity* 37: 880–892.
39. Cannons, J. L., L. J. Yu, D. Jankovic, S. Crotty, R. Horai, M. Kirby, S. Anderson, A. W. Cheever, A. Sher, and P. L. Schwartzberg. 2006. SAP regulates T cell-mediated help for humoral immunity by a mechanism distinct from cytokine regulation. *J. Exp. Med.* 203: 1551–1565.
40. McCausland, M. M., I. Yusuf, H. Tran, N. Ono, Y. Yanagi, and S. Crotty. 2007. SAP regulation of follicular helper CD4 T cell development and humoral immunity is independent of SLAM and Fyn kinase. *J. Immunol.* 178: 817–828.
41. Czar, M. J., E. N. Kersh, L. A. Mijares, G. Lanier, J. Lewis, G. Yap, A. Chen, A. Sher, C. S. Duckett, R. Ahmed, and P. L. Schwartzberg. 2001. Altered lymphocyte responses and cytokine production in mice deficient in the X-linked lymphoproliferative disease gene SH2D1A/DSHP/SAP. *Proc. Natl. Acad. Sci. USA* 98: 7449–7454.
42. Qi, H., J. L. Cannons, F. Klauschen, P. L. Schwartzberg, and R. N. Germain. 2008. SAP-controlled T-B cell interactions underlie germinal centre formation. *Nature* 455: 764–769.
43. Veillette, A., S. Zhang, X. Shi, Z. Dong, D. Davidson, and M.-C. Zhong. 2008. SAP expression in T cells, not in B cells, is required for humoral immunity. *Proc. Natl. Acad. Sci. USA* 105: 1273–1278.
44. Komori, H., H. Furukawa, S. Mori, M. R. Ito, M. Terada, M.-C. Zhang, N. Ishii, N. Sakuma, M. Nose, and M. Ono. 2006. A signal adaptor SLAM-associated protein regulates spontaneous autoimmunity and Fas-dependent lymphoproliferation in MRL-Faslpr lupus mice. *J. Immunol.* 176: 395–400.
45. Linterman, M. A., R. J. Rigby, R. K. Wong, D. Yu, R. Brink, J. L. Cannons, P. L. Schwartzberg, M. C. Cook, G. D. Walters, and C. G. Vinuesa. 2009. Follicular helper T cells are required for systemic autoimmunity. *J. Exp. Med.* 206: 561–576.
46. Keszei, M., C. Detre, W. Castro, E. Magelky, M. O'Keeffe, K. Kis-Toth, G. C. Tsokos, N. Wang, and C. Terhorst. 2013. Expansion of an osteopontin-expressing T follicular helper cell subset correlates with autoimmunity in B6.Sle1b mice and is suppressed by the H1-isoform of the Slamf6 receptor. *FASEB J.* 27: 3123–3131.
47. Detre, C., B. Yigit, M. Keszei, W. Castro, E. M. Magelky, and C. Terhorst. 2013. SAP modulates B cell functions in a genetic background-dependent manner. *Immunol. Lett.* 153: 15–21.
48. Pérez-Quintero, L.-A., R. Roncagalli, H. Guo, S. Latour, D. Davidson, and A. Veillette. 2014. EAT-2, a SAP-like adaptor, controls NK cell activation through phospholipase Cγ, Ca++, and Erk, leading to granule polarization. *J. Exp. Med.* 211: 727–742.